Journal of Solid State Chemistry 183 (2010) 2895–2902

Contents lists available at ScienceDirect

Journal of Solid State Chemistry

journal homepage: www.elsevier.com/locate/jssc

cis-trans Germanium chains in the intermetallic compounds $ALi_{1-x}In_xGe_2$ and $A_2(Li_{1-x}In_x)_2Ge_3$ (A=Sr, Ba, Eu)—experimental and theoretical studies

Tae-Soo You [1], Svilen Bobev *

Department of Chemistry and Biochemistry, University of Delaware, Newark, DE 19716, USA

ARTICLE INFO

Article history:
Received 19 July 2010
Received in revised form
16 September 2010
Accepted 26 September 2010
Available online 1 October 2010

Keywords:
Polar intermetallics
Crystal structure
Single-crystal X-ray diffraction
Electronic structure calculations

ABSTRACT

Two types of strontium-, barium- and europium-containing germanides have been synthesized using high temperature reactions and characterized by single-crystal X-ray diffraction. All reported compounds also contain mixed-occupied Li and In atoms, resulting in quaternary phases with narrow homogeneity ranges. The first type comprises $EuLi_{0.91(1)}In_{0.09}Ge_2$, $SrLi_{0.95(1)}In_{0.05}Ge_2$ and $BaLi_{0.99(1)}In_{0.01}Ge_2$, which crystallize in the orthorhombic space group *Pnma* ($BaLi_{0.9}Mg_{0.1}Si_2$ structure type, Pearson code *oP*16). The lattice parameters are a=7.129(4)–7.405(4) Å; b=4.426(3)–4.638(2) Å; and c=11.462(7)–11.872(6) Å. The second type includes $Eu_2Li_{1.36(1)}In_{0.64}Ge_3$ and $Sr_2Li_{1.45(1)}In_{0.55}Ge_3$, which adopt the orthorhombic space group *Cmcm* ($Ce_2Li_2Ge_3$ structure type, Pearson code *oC*28) with lattice parameters a=4.534(2)–4.618(2) Å; b=19.347(8)–19.685(9) Å; and c=7.164(3)–7.260(3) Å. The polyanionic sub-structures in both cases feature one-dimensional Ge chains with alternating Ge–Ge bonds in *cis*- and *trans*-conformation. Theoretical studies using the tight-binding linear muffin-tin orbital (LMTO) method provide the rationale for optimizing the overall bonding by diminishing the π–p delocalization along the Ge chains, accounting for the experimentally confirmed substitution of Li for In.

1. Introduction

During our systematic investigations on the composition–structure–property relationships of novel intermetallic compounds, we have successfully synthesized and characterized several novel kinds of germanides. So far, we have reported on the new homologous series of $A_{2[n+m]}In_{2n+m}Ge_{2[n+m]}$, where A stands for Ca, Sr, Eu, and Yb [1]. Their crystal structures are best viewed as intergrowths of and Mo_2FeB_2- and TiNiSi-like fragments in different ratios/stacking sequences. For example, we synthesized and structurally characterized $(Eu_{1-x}Ca_x)_4In_3Ge_4$ ($0.3 \le x \le 0.7$), when n=1 and m=1; $(Eu_{1-x}Ca_x)_3In_2Ge_3$ ($0.7 \le x \le 0.9$) for n=1 and m=2; and $(Ca_{1-x}Yb_x)_8In_5Ge_8$ ($x \approx 0.4$) for n=1 and m=3, respectively, [1]. Notably, all members of this series were found to exist only with mixed cations [1]. Then, based on the established structural trends, we attempted to extend the series and to synthesize higher order homologues by employing different combinations of alkaline-earth metals. These efforts led to the discovery of other new phases—$(Sr_{1-x}Ca_x)_5In_3Ge_6$/$(Eu_{1-x}Yb_x)_5In_3Ge_6$ ($x \approx 0.7$) and $(Sr_{1-x}Ca_x)_3In_2Ge_4$/ $(Sr_{1-x}Yb_x)_3In_2Ge_4$ ($0.4 \le x \le 0.5$), which were reported by us very recently [2]. The latter structures are not directly related to the structures from the $A_{2[n+m]}In_{2n+m}Ge_{2[n+m]}$ series. In addition to an $InGe_4$ tetrahedra, the $A_5In_3Ge_6$ structure features Ge_4 tetramers, while the $A_3In_2Ge_4$ structure is based on $InGe_4$ tetrahedra and Ge chains with an intricate topology of *cis*- and *trans*-bonds. Interestingly, similar Ge chains, where π-delocalization of the Ge 4*p*-orbitals must be considered, have been observed in the Li-containing compounds α-Sr_2LiGe_3 [3] and Eu_2LiGe_3 [4]. In these two instances, the special characteristics of the Li metal – its high ionic potential in particular – have been attributed as a key to the formation of such chains. In our previous study, we also noted that there was smeared electron density at one of the Ge sites (with trigonal planar environment), as well as some peculiarities in the electronic structure calculations (*e.g.*, $A_3In_2Ge_4$ is an electron-rich formula). Both suggested that a small disorder/pyramidalization at the Ge site could be concealed by the "average" structure, but might be critical to the optimization of the bonding by diminishing the π-conjugation along the germanium chains.

Following this hypothesis, we set out to investigate other possible structures, where similar Ge bonding patterns exist. Drawing on the structural analogies between the $^1_\infty[Ge_2]$ chains in $(Sr_{1-x}Ca_x)_3In_2Ge_4$ and the Li-containing Sr_2LiGe_3 [3], it was thought that small amounts of Li can be used to fine-tune the number of valence electrons in the compounds under consideration. These studies, however, did not yield the sought-after phases. Instead, as described next, the phases $ALi_{1-x}In_xGe_2$ ($0 \le x \le 0.1$) and $A_2(Li_{1-x}In_x)_2Ge_3$ ($x \approx 0.3$) were obtained (A=Sr, Ba, Eu). With this article, we present the single-crystal structures of these two types of closely related intermetallics, hereafter

* Corresponding author. Fax: +1 302 831 6335.
E-mail address: bobev@udel.edu (S. Bobev).
[1] Present address: Department of Chemistry, Chungbuk National University 410 Sungbong-ro, Heungduk-gu, Cheongju Chungbuk 361-763, South Korea.

0022-4596/$ - see front matter © 2010 Elsevier Inc. All rights reserved.
doi:10.1016/j.jssc.2010.09.041

dubbed for short as the "1-1-2" and "2-2-3" phases, respectively. We also discuss the correlations between the crystal structures with compositions, as well as the band structures, calculated using the tight-binding linear muffin-tin orbital (TB–LMTO–ASA) method [5].

2. Experimental

2.1. Synthesis

All manipulations were performed inside an argon-filled glove box or under vacuum. The starting materials – pure elements from Alfa or Aldrich (> 99.9%) – were used as received. All reactions were carried out using sealed Nb-ampoules. The reactant mixtures in the desired stoichiometric ratios were loaded into Nb-tubes, which were then sealed by arc-melting under an argon atmosphere. The welded Nb-ampoules were subsequently enclosed in fused silica tubes, which were flamed-sealed under vacuum to prevent oxidation upon heating to high temperature. The reaction mixtures were heated in muffle furnaces to 970 °C at a rate of 100 °C and kept at this temperature for 10 h, then slowly cooled to 650 °C, where the reactions were annealed for a week. Final step – cooling to room temperature – was done by turning the furnace off. The products of such reactions were bar or needle-shaped crystals with silver luster. Based on powder, as well as single-crystal X-ray diffraction, both the Eu–Li–In–Ge and the Sr–Li–In–Ge reactions produced mixtures of the "1-1-2" and the "2-2-3" phases with some elemental In left. All attempts to synthesize a single-phase material in each case were unsuccessful so far—given the close compositional and structural similarities between the "1-1-2" and the "2-2-3" phases, this is not very surprising. The Ba–Li–In–Ge reactions produced complex mixtures of $BaGe_2$ [6], $BaLi_{1-x}In_xGe_2$, leftover In, and another hitherto unknown $BaLi_2Ge_4$ phase with a new rhombohedral structure (s.g. $R\bar{3}m$; $a=4.582(2)$ Å; $c=26.287(18)$ Å), which will be the topic of a subsequent article. Despite the repeated tries, $CaLi_{1-x}In_xGe_2$, $YbLi_{1-x}In_xGe_2$, $Ca_2(Li_{1-x}In_x)_2Ge_3$, or $Yb_2(Li_{1-x}In_x)_2Ge_3$, isostructural to the two title phases, could not be prepared. Instead, these reactions yielded some known binaries and the ternary/quaternary phases Yb_8LiGe_{13} [7] and $Ca_2LiInGe_2$ [8], respectively.

We must also note here that our stoichiometric reactions of Sr and Ba with Li and Ge, i.e., without using In, produced $SrLiGe_2$ and $BaLiGe_2$; however, we were unsuccessful in producing pure ternary $Sr_2Li_2Ge_3$ and $Ba_2Li_2Ge_3$. Stoichiometric reactions of Eu, Li and Ge in Nb-tubes also did not afford the targeted $EuLiGe_2$ and $Eu_2Li_2Ge_3$ phases. Instead, these experiments led to the identification of the new line compound $EuLiGe_2$, adopting the $CaLiSi_2$ type structure [9]. Apparently, as discussed at length in the last section of this paper, the random substitution of Li with In (or Mg) taking place in both phases is very important, particularly for the formation of the "2-2-3" phases. These arguments are further supported by the synthesis of $Eu_2Li_{1.11(1)}Mg_{0.89}Ge_3$, a Mg-substituted version of $Eu_2Li_{1.36(1)}In_{0.64}Ge_3$, which was also structurally characterized as part of this study. Notice that this phase is virtually identical to $Eu_2Li_{1.16(1)}Mg_{0.84}Ge_3$, reported in 2004 by Xie and Nesper [4], and even though a series of reactions with nominal compositions $Eu_2(Li_{1-x}In_x)_2Ge_3$ and $Eu_2(Li_{1-x}Mg_x)_2Ge_3$ ($0 \le x \le 1$) were performed, only the presented compounds were synthesized. Such observations are suggestive of negligible phase widths in both cases.

2.2. X-ray crystallography

X-ray powder diffraction patterns were taken at room temperature on a Rigaku MiniFlex powder diffractometer using Cu $K\alpha$ radiation ($\theta-\theta$ scan mode with a step-size of 0.05 s. The diffractometer was enclosed and operated inside a nitrogen-filled glove box to handle air and moisture sensitive materials. Typical runs included $\theta-\theta$ scans with scan steps of 0.05° and 5 s/step counting time. JADE 6.5 was used for data analysis. Powder patterns collected for specimens kept under inert atmosphere and exposed to air (for different periods of time) suggested that the polycrystalline materials remain unchanged for at least 72 h.

Single-crystal X-ray diffraction data were collected at 200 K on a Bruker SMART CCD-based diffractometer. First, several crystals from each batch were selected and checked for quality by rapid scans before the best ones were chosen for further analysis. Monochromated Mo $K\alpha_1$ radiation ($\lambda=0.71073$ Å) was used, and data collections were handled in batch runs at different ω and ϕ angles, controlled by the *SMART* software [10]. Frame width was 0.3–0.4° in ω and θ with data acquisition rate of 8–12 s/frame. The angular range in 2θ was up to *ca.* 60°. The *SAINT* program was used to extract and correct intensities for Lorentz and polarization effects [11]. The structure factors were sorted and merged by the program *XPREP* in the *SHELXTL* software package [12], which was also employed in the space group determination. Semi-empirical absorption correction based on equivalents was applied using *SADABS* [13]. The structures were solved by direct methods and refined to convergence by full matrix least-squares methods on F^2. Refined parameters included the scale factor, the atomic positions with anisotropic displacement parameters, extinction coefficient (not for all), and occupancy factors for the mixed positions.

On this note, we draw attention to the fact that in all cases, the Li sites (in both structure types) were refined as statistical mixtures with either In or Mg. The reasons for refining the structures in such manner were: (1) the electron densities at the Li sites were found to be higher than what was expected for Li, which indicated that there was a partial occupation by a heavier element at the Li site. For $ALi_{1-x}In_xGe_2$ (A=Eu, Sr, Ba), the site occupation factors were *ca.* 180%, 90% and 16% greater than fully occupied Li, leading to refined formulas $EuLi_{0.91(1)}In_{0.09}Ge_2$, $SrLi_{0.95(1)}In_{0.05}Ge_2$ and $BaLi_{0.99(1)}In_{0.01}Ge_2$, respectively [14]. For $Sr_2(Li_{1-x}In_x)_2Ge_3$, $Eu_2(Li_{1-x}In_x)_2Ge_3$, and $Eu_2(Li_{1-x}Mg_x)_2Ge_3$, the Li admixtures with In or Mg were even more discernable than those in the "1-1-2" phases, yielding refined formulas $Sr_2Li_{1.45(1)}In_{0.55}Ge_3$, $Eu_2Li_{1.36(1)}In_{0.64}Ge_3$, and $Eu_2Li_{1.11(1)}Mg_{0.89}Ge_3$, respectively. (2) Pure ternary $EuLiGe_2$ or $A_2Li_2Ge_3$ compounds (A=Sr, Eu) could not be synthesized. Both points mentioned above suggest that likely, there is an electronic effect at play here, whereby the small Li–In or Li–Mg admixtures augment the number of valence electrons to their optimal levels to stabilize the polyanionic networks (*vide infra*).

In the final refinement cycles, the atomic coordinates were standardized with the aid of *STRUCTURE TIDY* [16]. Relevant crystallographic information for all data collections is given in Tables 1 and 2. Final positional and equivalent isotropic displacement parameters, and selected interatomic distances for representative members of the "1-1-2" and "2-2-3" structures are listed in Tables 3 and 4, respectively. The data for the remaining structures are provided in the supporting information. CIFs have also been deposited with Fachinformationszentrum Karlsruhe, 76344 Eggenstein-Leopoldshafen, Germany, (fax: (49) 7247-808-666; e-mail: crysdata@fiz.karlsruhe.de) with depository Nos.: CSD-421973 for $EuLi_{0.91(1)}In_{0.09}Ge_2$, CSD-421974 for $SrLi_{0.95(1)}In_{0.05}Ge_2$, CSD-421975 for $BaLi_{0.99(1)}In_{0.01}Ge_2$, CSD-421976 for $Eu_2Li_{1.36(1)}In_{0.64}Ge_3$, CSD-421977 for $Sr_2Li_{1.45(1)}In_{0.55}Ge_3$, and CSD-421978 for $Eu_2Li_{1.11(1)}Mg_{0.89}Ge_3$.

2.3. Electronic structure calculations

Tight-binding, linear muffin-tin orbital (TB-LMTO) calculations [5] were carried out using the LMTO47 program [17]. This

Table 1
Selected single-crystal data collection and structure refinement parameters for $ALi_{1-x}In_xGe_2$ ("1-1-2" phases; A=Sr, Ba, and Eu).

Empirical formula	$SrLi_{0.95(1)}In_{0.05}Ge_2$	$BaLi_{0.99(1)}In_{0.01}Ge_2$	$EuLi_{0.91(1)}In_{0.09}Ge_2$
Formula weight, Z=4	245.13	290.00	314.06
Crystal system		Orthorhombic	
Space group		*Pnma*, No. 62	
Temperature (K)		200 K	
Unit cell dimensions (Å)	a=7.162(3)	a=7.405(4)	a=7.129(4)
	b=4.4677(19)	b=4.638(2)	b=4.426(3)
	c=11.547(5)	c=11.872(6)	c=11.462(7)
Volume (Å^3)	369.5(3)	407.8(4)	361.7(4)
Density (calculated, g/cm^3)	4.407	4.724	5.767
Absorption coefficient (cm^{-1})	305.77	239.74	339.31
Data/restraints/parameters	516/0/26	551/0/27**	508/0/26
R^* indices [$I>2\sigma_I$]	$R1$=0.0442	$R1$=0.0403	$R1$=0.0265
	w$R2$=0.0898	w$R2$=0.0845	w$R2$=0.0526
R^* indices [all data]	$R1$=0.0721	$R1$=0.0655	$R1$=0.0374
	w$R2$=0.1001	w$R2$=0.0929	w$R2$=0.0564
Goodness-of-fit on F^2	1.105	1.041	1.070
Largest diff. peak/hole (e/Å^3)	2.47/−1.21	2.03/−2.26	2.12/−1.34

* $R1=\sum||F_o|-|F_c||/\sum|F_o|$; $wR2=[\sum[w(F_o^2-F_c^2)^2]/\sum[w(F_o^2)^2]]^{1/2}$, where $w=1/[\sigma^2F_o^2+(A\cdot P)^2+B\cdot P.]$, and $P=(F_o^2+2F_c^2)/3$; A and B – weight coefficients.
** The extra variable is the extinction coefficient: 0.0020(5).

Table 2
Selected single-crystal data collection and structure refinement parameters for the "2-2-3" phases $A_2(Li_{1-x}In_x)_2Ge_3$ (A=Sr and Eu) and $Eu_2(Li_{1-x}Mg_x)_2Ge_3$.

Empirical formula	$Sr_2Li_{1.45(1)}In_{0.55}Ge_3$	$Eu_2Li_{1.37(1)}In_{0.63}Ge_3$	$Eu_2Li_{1.10(1)}Mg_{0.90}Ge_3$
Formula weight, Z=4	466.22	604.07	551.20
Crystal system		Orthorhombic	
Space group		*Cmcm*, no. 63	
Temperature (K)		200 K	
Unit cell dimensions (Å)	a=4.618(2)	a=4.534(2)	a=4.5618(13)
	b=19.685(9)	b=19.347(8)	b=19.442(6)
	c=7.260(3)	c=7.164(3)	c=7.208(2)
Volume (Å^3)	660.0(5)	628.4(5)	639.2(3)
Density (calculated, g/cm^3)	4.692	6.385	5.727
Absorption coefficient (cm^{-1})	312.98	359.78	332.22
Data/restraints/parameters	529/0/27	518/0/27	514/0/27
R^* indices [$I>2\sigma_I$]	$R1$=0.0305	$R1$=0.0196	$R1$=0.0209
	w$R2$=0.0605	w$R2$=0.0429	w$R2$=0.0433
R^* indices [all data]	$R1$=0.0404	$R1$=0.0239	$R1$=0.0267
	w$R2$=0.0633	w$R2$=0.0450	w$R2$=0.0446
Goodness-of-fit on F^2	1.018	1.089	1.001
Largest diff. peak/hole (e/Å^3)	0.96/−1.42	0.82/−1.63	1.23/−1.78

* $R1=\sum||F_o|-|F_c||/\sum|F_o|$; $wR2=[\sum[w(F_o^2-F_c^2)^2]/\sum[w(F_o^2)^2]]^{1/2}$, where $w=1/[\sigma^2F_o^2+(A\cdot P)^2+B\cdot P]$, and $P=(F_o^2+2F_c^2)/3$; A and B—weight coefficients.

Table 3
Atomic coordinates and equivalent isotropic displacement parameters (U_{eq})[a] from single-crystal structure refinements for $SrLi_{0.95(1)}In_{0.05}Ge_2$ and $Sr_2Li_{1.45(1)}In_{0.55}Ge_3$, chosen as representatives of the "1-1-2" and "2-2-3" phases.

Atom	*Wyck*off site	x	y	z	U_{eq} (Å^2)	Occup.
$SrLi_{0.95(1)}In_{0.05}Ge_2$						
Sr	4*c*	0.1373(2)	1/4	0.8558(1)	0.012(1)	1
M[b]	4*c*	0.130(1)	1/4	0.5598(9)	0.011(3)	0.955(4)/0.045
Ge1	4*c*	0.0363(2)	1/4	0.3387(1)	0.012(1)	1
Ge2	4*c*	0.1905(2)	1/4	0.1438(1)	0.012(1)	1
$Sr_2Li_{1.45(1)}In_{0.55}Ge_3$						
Sr1	4*c*	0	0.3441(1)	1/4	0.017(1)	1
Sr2	4*c*	0	0.5546(1)	1/4	0.012(1)	1
M[b]	8*f*	0	0.1912(1)	0.0589(2)	0.015(1)	0.726(2)/0.274
Ge1	8*f*	0	0.0568(1)	0.5769(1)	0.012(1)	1
Ge2	4*c*	0	0.7218(1)	1/4	0.014(1)	1

[a] U_{eq} is defined as one third of the trace of the orthogonalized U_{ij} tensor.
[b] Refined as a statistical mixture of Li and In.

package employs the atomic sphere approximation (ASA) method, in which space is filled with overlapping Wigner–Seitz (WS) atomic spheres [18]. The symmetry of the potential is considered spherical inside each WS sphere, and a combined correction is used to take into account the overlapping part [19]. The radii of WS spheres were obtained by requiring that the overlapping

potential be the best possible approximation to the full potential, and were determined by an automatic procedure [19]. This overlap should not be too large, because the error in kinetic energy introduced by the combined correction is proportional to the fourth power of the relative sphere overlap. The WS radii are as follows: for the "1-1-2" series: Sr=2.29 Å, Li=1.60 Å, and Ge=1.43 Å; and for the "2-2-3" series: Sr=2.13–2.18 Å, Li=1.49 Å, and Ge=1.50–1.81 Å. Exchange and correlation were treated by the local density approximation (LDA) [20]. All relativistic effects, except spin-orbit coupling, were taken into account by using a scalar relativistic approximation.

The density of states (DOS) plots are presented herein with the Fermi level set as a reference point at 0 eV. In order to evaluate various orbital interactions, the crystal orbital Hamilton populations (COHP) [21] were also calculated. The *k*-space integrations were conducted by the tetrahedron method [22], and the self-consistent charge density was obtained using 180–216 irreducible *k*-points in the Brillouin zone.

3. Results and discussion

3.1. "1-1-2" Phase

The three compounds $EuLi_{0.91(1)}In_{0.09}Ge_2$, $SrLi_{0.95(1)}In_{0.05}Ge_2$ and $BaLi_{0.99(1)}In_{0.01}Ge_2$ crystallize in the orthorhombic space group *Pnma* ($BaLi_{0.9}Mg_{0.1}Si_2$ structure type [23]), with Pearson code *oP*16 [24]. The structure could also be assigned with the $ScRhSi_2$ structure type [24,25], if the Rh site is occupied by one of the Ge atoms and the Si2 position is taken by the Li atom. There are 4 crystallographically unique atomic positions in the asymmetric unit (Table 2). The overall crystal structure can be described as one-dimensional (1-D) Ge chains with a basic repeating unit of $(ct)_n$, where *c* refers to the *cis*- and *t* refers to the *trans*-conformation [4] propagating along the *a*-axis, with cations filling the space between these polyanionic fragments (Fig. 1).

The $^1_\infty[Ge_2]$ chains in the "1-1-2" phase have exactly the same topology as those in LT-LaGe (LT=low-temperature) [26], although they are slightly "kinked" and do not have mirror plane symmetry in the direction perpendicular to the chain, as in LT-LaGe. After recognizing this relationship, the crystal structure of the "1-1-2" phase can be derived from the LT-LaGe type structure, which in turn is a derivative of the AlB_2 type [24]. To illustrate this idea, let us consider hypothetical AGe_2 phase with honeycomb $^2_\infty[Ge_2]$ layers, as shown in Fig. 2(a). The *A*-cations form trigonal prisms around each Ge, forming slabs in a plane perpendicular to the hexagonal axis. Upon a patterned removal of half of the Ge atoms, in a way that $^1_\infty[Ge_2]$ chains of alternating *cis*- and *trans*-bonds are left behind, a half of the A_6-trigonal prisms become empty. The arrangement of the empty and the filled prisms can be described as puckered "layers", running parallel to the direction of the plot, as shown in Fig. 2(b). One can readily see that the latter represents the structure of LT-LaGe [26]. Parenthetically, a different way of removing half of the Ge atoms from the same $^2_\infty[Ge_2]$ layers will yield $^1_\infty[Ge_2]$ zig–zag chains, which are the same as in the high-temperature LaGe polymorph (FeB type) [24,27] or in an SrGe (CrB type) [24,28].

The same idea allows us to account for at least two other structures with similar characteristics—these are the title "1-1-2" phase and the previously mentioned α-Sr_2LiGe_3 [3] and Eu_2LiGe_3 [4]. Hence, by reformulating the monogermanide as A_2Ge_2 (or rather $AA'Ge_2$, where *A* stands for the cations within the chain, and *A'* stands for the cations between the chains) and applying an imaginary Li substitution for half of the cations (the ones labeled *A'*), we easily obtain the "1-1-2" structure with the distorted $(ct)_n$ chains as shown in Fig. 2(c). Notice that the Li-substitution occurs only at the *cis*-position on the $^1_\infty[Ge_2]$ chain causing the latter to distort a bit at this position—evidently the effect of smaller and highly polarizing Li^+ cation. The size difference between the two types of cations can explain this preferential replacement—the much smaller Li^+ is 5-coordinated to Ge atoms in the *cis*-position,

Table 4
Selected bond distances (in Å) for $SrLi_{0.95(1)}In_{0.05}Ge_2$ and $Sr_2Li_{1.45(1)}In_{0.55}Ge_3$, chosen as representatives of the "1-1-2" and "2-2-3" phases.

$SrLi_{0.95(1)}In_{0.05}Ge_2$		$Sr_2Li_{1.45(1)}In_{0.55}Ge_3$	
Atomic pair	Distance	Atomic pair	Distance
Ge1–Ge2 (1 ×)	2.485(2)	Ge1–Ge1 (1 ×)	2.498(2)
Ge1–Ge2 (1 ×)	2.508(2)	Ge1–Ge1 (1 ×)	2.514(2)
Ge1–*M*[a] (1 ×)	2.64(1)	Ge1–*M*[a] (2 ×)	2.824(2)
Ge1–*M*[a] (2 ×)	2.790(7)	Ge2–*M*[a] (4 ×)	2.760(1)
Ge2–*M*[a] (2 ×)	2.753(6)	Ge2–*M*[a] (2 ×)	2.822(2)
		M–*M*[a] (1 ×)	2.774(3)

[a] Refined as mixed-occupied Li–In site.

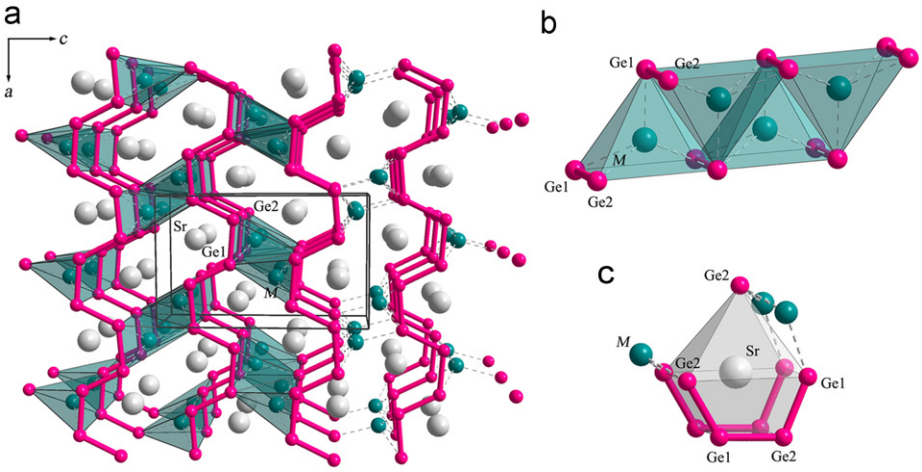

Fig. 1. (a) Combined ball-and-stick and polyhedral representations of the crystal structure of the orthorhombic $SrLi_{0.95(1)}In_{0.05}Ge_2$ ("1-1-2" phase), viewed down the *b*-axis. The unit cell is outlined. The infinite $^1_\infty[Ge_2]$ chains with *cis*- and *trans*-conformation in the repeating unit of $(ct)_n$ are highlighted. (b) A close up view, emphasizing the connectivity of the pyramidal $[Ge_5]$-fragments, centered by Li. (c) Coordination polyhedron of the alkaline-earth (or Eu^{2+}) cation.

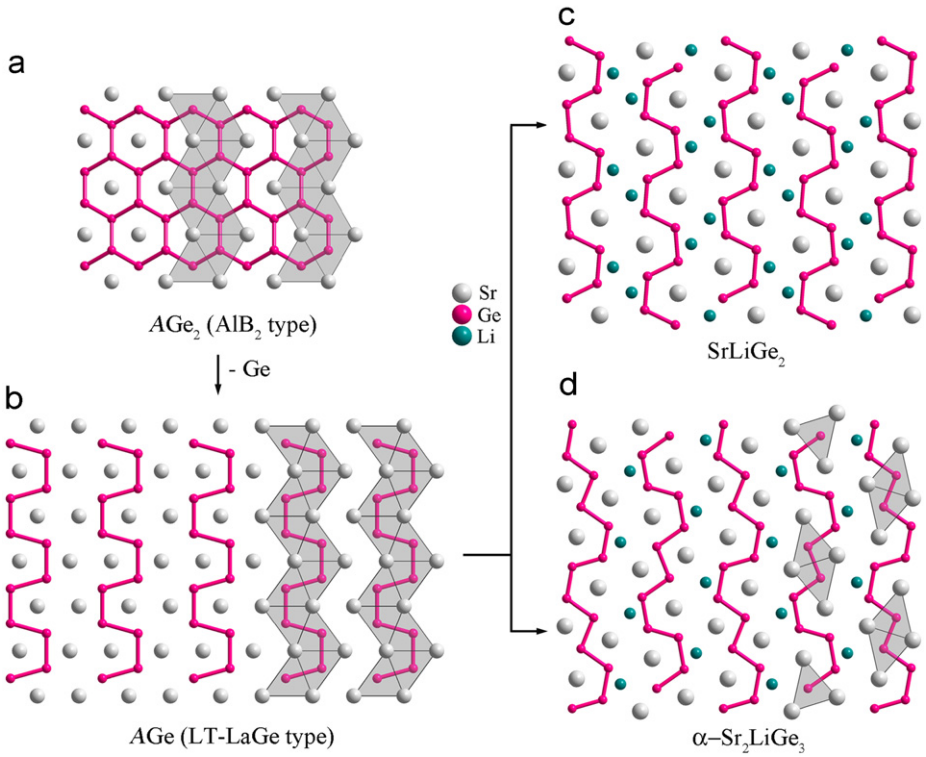

Fig. 2. Schematic illustration of the structural relationship between the hypothetical $SrGe_2$ (AlB_2 type) (a), and the hypothetical SrGe (LT-LaGe type) (b). Further parallels can be drawn between the latter and $SrLiGe_2$ (c) on one side and α-Sr_2LiGe_3 (d) on the other. See the text for more details.

while the larger A^{2+} cations are 9-coordinated by Ge atoms in both *cis*- and *trans*-positions. In another cut-and-paste experiment (Fig. 2(d)), the *A*Ge formula can be rewritten as A_3Ge_3, then a 1/3 of the *A*-cations can be substituted by an Li, which accounts for the α-Sr_2LiGe_3 structure (the "2-1-3" phase) [3]. In this case, unlike the "1-1-2" structure, the resultant Ge chains have a more complicated repeating unit, i.e., $(tttctc)_n$. The distortion of the Ge chains can be understood with respect to the formal charges assigned to each Ge atom, and we will discuss this in the bonding and electronic structure section.

The *cis*- and *trans*- Ge–Ge bonds in $EuLi_{0.91(1)}In_{0.09}Ge_2$ are virtually identical with distances d(Ge–Ge)=2.506(2) Å. The observed Ge–Ge distances for the two kinds of bonds in $SrLi_{0.95(1)}In_{0.05}Ge_2$ and $BaLi_{0.99(1)}In_{0.01}Ge_2$ show significant differences: 2.485(2)/2.508(2) Å, and 2.479(2)/2.534(2) Å, respectively. This clearly can be attributed to the different amount of an In, which alters not only the overall electron count (*vide infra*), but also influences the local bonding. These distances are slightly longer than the contacts in an elemental Ge (2.45 Å, four-bonded) [29], but are significantly shorter than the Ge–Ge distances within the zig–zag $^1_\infty[Ge_2]$ chains in SrGe (ca. 2.63 Å) [28], and the $(ct)_n$ $^1_\infty[Ge_2]$ chains in LT-LaGe (d(Ge–Ge)=2.621/2.779 Å) [26], where each Ge atom is also two-bonded. Another useful comparison can be made with Eu_2LiGe_3 [4], where Ge chains with *cis*- and *trans*-bonds are also present. There are four different Ge–Ge distances in Eu_2LiGe_3, and among them, two of the Ge–Ge bonds that are "coordinated" to Li atoms are shorter (2.461(2) and 2.491(1) Å) than the other two Ge–Ge bonds that do not have adjacent Li atoms (2.579(1) and 2.612(2) Å) [4]. The same holds true for an $ALi_{1-x}In_xGe_2$, where the *cis*-bonds are up to 2% shorter than the *trans*-bonds. The cause of this effect, as discussed by Nesper et al. [4], is the special "zwitter" role of Li. It is not only donating a valence electron to the anionic framework, acting as a cation, but also contributes to the covalent interactions within the polyanionic network. In our "1-1-2" compounds, the Li atoms also participate in covalent bonding with Ge, forming $[LiGe_2]$ polyanionic networks with corresponding Li–Ge distances of 2.64(1)–2.73(2) Å (Fig. 1, Tables 4 and S2). Not surprisingly, therefore, the values for Ge–Ge bonds we are reporting here are close to those for known structures with 3-bonded Ge (formally Ge^{1-}), such as $EuGe_2$ [30], $CaGe_2$ [31], Sm_3Ge_5 [32], and $Ca_2LiInGe_2$ [8] (2.528–2.557 Å). However, since the Li atoms can be partially substituted by an In, the electron count in an $ALi_{1-x}In_xGe_2$ can be varied, and the covalent contribution can be "tuned". Another direct effect of this tunability can be seen by comparing the length of the *cis*- and the *trans*-bonds on going from the Eu-, through the Sr-, to the Ba-phase (Table 3). Notice how the differential between the Ge–Ge distances widens in the same order, which can be correlated with decreasing of the In content, i.e., an increase of the valence electron count. The above indicates that π-delocalization of the Ge 4*p*-orbitals must be considered when rationalizing the electronic structures.

This analysis on the Ge–Ge distances indicates that the notion of a π-contribution to the Ge–Ge interactions is of an essence here. Evidently, a direct analogy with the double-bonds observed in several molecular species, i.e., $H_2Ge{=}GeH_2$ [33] with d(Ge–Ge)=2.29 Å and $R_2Ge{=}GeR_2$ (R=2,5-tBu$_2$C$_6$H$_3$) [34] with d(Ge–Ge)=2.36 Å, is not possible. Nonetheless, the p–π delocalization is clear from the *ab-initio* electronic structure calculations presented later on, as well as the Hückel treatment published by DiSalvo et al. [15]. In addition, other examples of conjugated chains with *cis*- and *trans*-Ge-bonds, such as Eu_2LiGe_3 [4], have also been analyzed at length.

3.2. "2-2-3" Phase

The compounds $Eu_2Li_{1.36(1)}In_{0.64}Ge_3$, $Eu_2Li_{1.11(1)}Mg_{0.89}Ge_3$, and $Sr_2Li_{1.45(1)}In_{0.55}Ge_3$ crystallize in the orthorhombic space group

Cmcm ($Ce_2Li_2Ge_3$ type, Pearson code *oC*28) [24,35] with 5 crystallographically unique atomic positions in the asymmetric unit (Tables 2 and 3). Several other Li-containing intermetallics with the general formula $A_2(Li_{1-x}Mg_x)_2Tt_3$ (A=Sr, Eu; Tt=Si, Ge; $x \approx 0.5$) [36,37] are also known, and they are isostructural to an $A_2(Li_{1-x}In_x)_2Ge_3$ ($x \approx 0.3$). Since this structure type has been described elsewhere [35], in the next paragraph, we will focus our attention on the Ge and Li bondings, emphasizing some structural trends in connection with the electronic structure.

In the "2-2-3" structure (Fig. 3(a)), there are two different types of Ge atoms: one forms the $^1_\infty[Ge_2]$ chains with a basic repeating unit of $(ct)_n$, similar to those in the "1-1-2" phase, and the other one which is isolated. The *cis–trans* chains here are very similar to those in the "1-1-2" phase, except that they are more symmetric (as quantified by the Ge–Ge–Ge angles, for example 115.89(3)° in $Sr_2Li_{1.45(1)}In_{0.55}Ge_3$ vs. 111.46(6)°/120.81(6)° in $SrLi_{0.95(1)}In_{0.05}Ge_2$, and 115.88(3)° in $Eu_2Li_{1.36(1)}In_{0.64}Ge_3$ vs. 109.61(5)/120.98(5)° in $EuLi_{0.91(1)}In_{0.09}Ge_2$, respectively). The difference can be clearly attributed to the fact that the Ge atoms are all located at the centers of trigonal prisms, formed by six strontium or europium atoms. Li atoms in the "2-2-3" structure are also fulfilling two roles, as previously discussed for the "1-1-2" phase. Here, Li atoms (mixed with an In or an Mg) are covalently bound to the Ge1 atoms from the chain with Li–Ge distances 2.731(2)–2.824(1) Å. At the same time, Li atoms tightly coordinate the isolated Ge2 atoms having a formal charge of 4–, with an Li–Ge separation in the range 2.727(1)–2.821(2) Å.

The observed Ge–Ge distances vary between 2.475(1) and 2.502(1) Å for $Eu_2Li_{1.36(1)}In_{0.64}Ge_3$, between 2.472(1) and 2.506(1) Å for $Eu_2Li_{1.11(1)}Mg_{0.89}Ge_3$, and between 2.498(1) and 2.514(1) Å for $Sr_2Li_{1.45(1)}In_{0.55}Ge_3$, respectively. These values are comparable to the ones seen for the "1-1-2" compounds (*vide infra*), $Eu_2Li_{1.16(1)}Mg_{0.84}Ge_3$ (d(Ge–Ge)=2.482(2)–2.513(2) Å) and $Sr_2Li_{0.94(1)}Mg_{1.06(1)}Ge_3$ (d(Ge–Ge)=2.496(1)–2.527(1) Å) [36], as well as those in $Ce_2Li_2Ge_3$ (d(Ge–Ge)=2.494(1)–2.521(1) Å) [35]. Interestingly, except for $Eu_2Li_{1.11(1)}Mg_{0.89}Ge_3$, in all other compounds, the *cis*-bond is a bit longer than the Ge–Ge bond in the *trans*-conformation.

There are two cationic positions in the "2-2-3" phase (Fig. 3(b)). The *A*1-site is 12-coordinated: 10 atoms (6 Ge and 4 Li mixed sites) form a pentagonal prism, and two additional Li's cap two of the rectangular faces. The *A*2-site is surrounded by a total of 13 neighbors, including 9 Ge's and 4 Li's. The Li-site (statistically mixed with In or Mg) is located near the center of a distorted tetrahedron of Ge atoms. These $LiGe_4$-tetrahedra are edge-shared to form layers running along the *ac*-plane (Fig. 3(c)).

3.3. Bonding and electronic structure

To understand the chemical bonding and the electronic structures of the two types of phases, band-structure calculations were conducted using the TB-LMTO-ASA method [5]. For a practical reason, we used $SrLiGe_2$ without any mixed-occupation of Li and In for the "1-1-2" phase.

DOS and COHP curves are plotted in Fig. 4. As seen from the plot of the total density of states (TDOS), there is no band gap at the Fermi level, which is located near the local energy minimum corresponding to 44 e^-/cell. The large orbital mixing between Ge *p*-orbitals and both Sr and Li states in the vicinity of the Fermi level is a testament to the previously stated fact that the cations participate in covalent interactions with the polyanionic network and should not be regarded as just electron donors. This point is particularly important for the Li–Ge interactions, whose covalent character is also evident from their COHP curves. Since there are two inequivalent Ge–Ge bonds (*cis*- and *trans*-), they are differentiated and plotted separately in the middle of Fig. 4.

If we bring up the formal charge of each Ge based on the Zintl–Klemm concept [38], an $SrLiGe_2$ should be rationalized as $(Sr^{2+})(Li^+)(Ge_2^{3-})$ [15], although each Ge is two-bonded and should have a formal charge q=2–. In the formulation above, Ge atom ought to be assigned a formal charge q=1.5–/each in order to achieve electroneutrality [39]. This value is higher than the expected formal charge of 1– for Ge in polyacetylene-like $^1_\infty[Ge_2]^{2-}$ chain [23]. Hence, a structure description with at least a partial double-bond character of the Ge–Ge interactions is necessary in order to conform to the octet rule. Such conclusion is in line with the previously noted signs of π-delocalization along the $^1_\infty[Ge_2]$ chain, discussed alongside the comparative analysis of the Ge–Ge distances (*vide supra*). Indeed, the partial population of the π^* Ge-states is indicated on the COHP curves (Fig. 4). In addition, from the COHP analysis of the *cis*- and *trans*-bonds, we see that both will respond differently to small changes in the energy of the Fermi level—this explains the different *cis*- and *trans*-bonds in $BaLi_{0.99(1)}In_{0.01}Ge_2$ (44.1 e^-/cell) vs. the slightly electron-richer $EuLi_{0.91(1)}In_{0.09}Ge_2$ (44.7 e^-/cell), where both bonds are nearly equal. We also calculated the band structure of LT-LaGe [26], which also features *cis*- and *trans*-chains (in spite of the formal charge q=3– per Ge atom). This was done in order to compare the Ge–Ge COHP curves, and the results confirming the anti-bonding character are displayed in supporting information (Figure S1).

For the "2-2-3" phase, an idealized composition "$Sr_2Li_2Ge_3$" was used without any Li/In mixed-occupation, using atomic positions and lattice parameters taken from $Sr_2Li_{1.45(1)}In_{0.55}Ge_3$ (Table 1). As shown in Fig. 5, the total density of states (TDOS) at

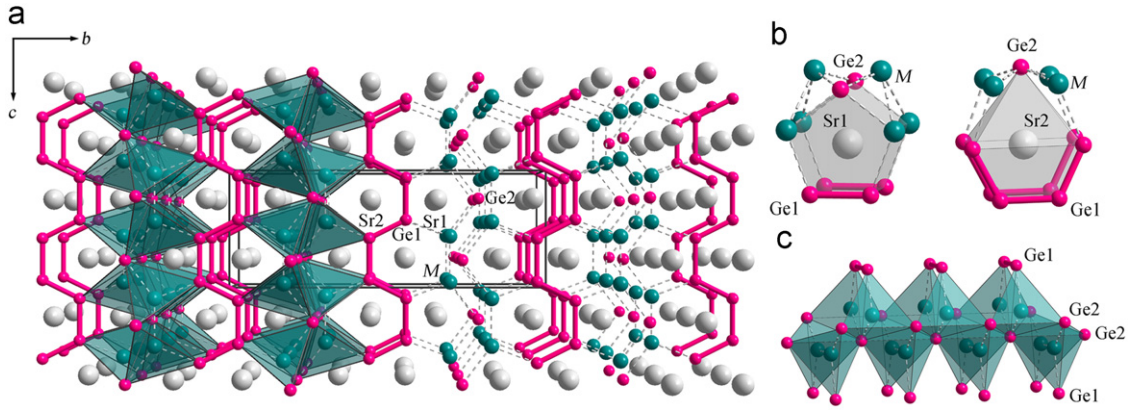

Fig. 3. (a) Combined ball-and-stick and polyhedral representations of the crystal structure of the orthorhombic $Sr_2(Li_{1-x}In_x)_2Ge_3$ ("2-2-3" phase), viewed down the *a*-axis. The unit cell is outlined. (b) Coordination polyhedra of the two alkaline-earth (or Eu^{2+}) cations. (c) A close up view emphasizing the edge-shared tetrahedral [$LiGe_4$] chains.

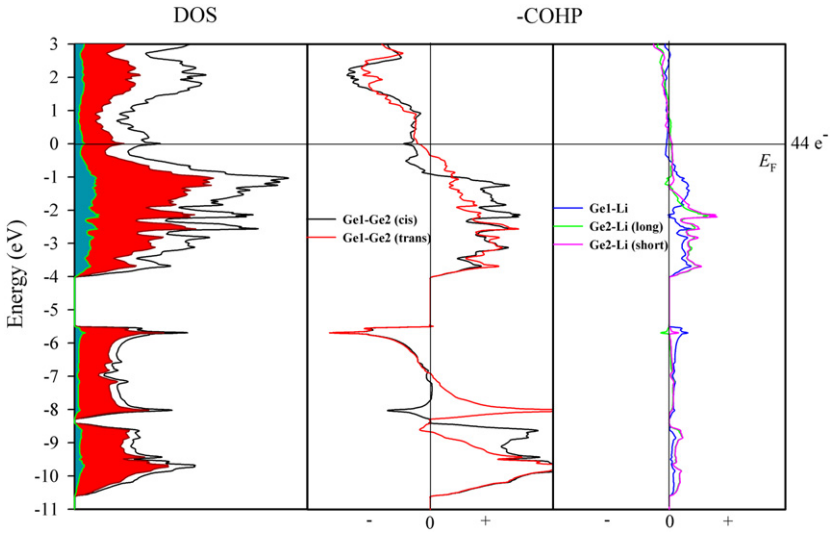

Fig. 4. DOS and COHP curves for $SrLiGe_2$ ("1-1-2" phase). Total DOS curves are shown with a solid line; partial DOS curves of Sr, Ge, and Li are represented, respectively, by the area shaded in white, red, and green. E_F (solid line) is the energy reference at 0 eV. The local DOS minima (dashed line) and the corresponding number of valence electrons are also displayed. In the –COHP curves, the "+" values are bonding interactions; the "–" values are antibonding interactions, respectively.

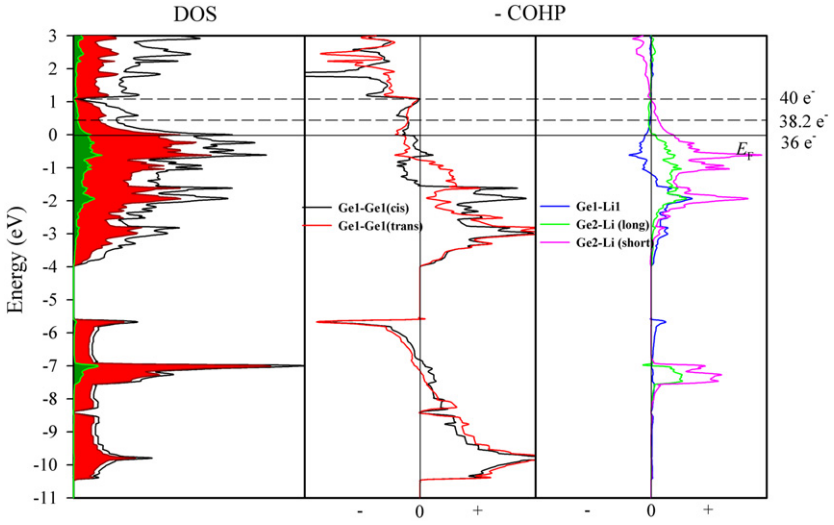

Fig. 5. DOS and COHP curves for $Sr_2Li_2Ge_3$ ("2-2-3" phase). Total DOS curves are shown with a solid line; partial DOS curves of Sr, Ge, and Li are represented, by the area shaded in white, red, and green, respectively. E_F (solid line) is the energy reference at 0 eV. The local DOS minima (dashed line) and the corresponding number of valence electrons are also displayed. In the –COHP curves, the "+" values are bonding interactions; the "–" values are antibonding interactions, respectively. (For interpretation of the references to color in this figure legend, the reader is referred to the web version of this article.)

the Fermi level corresponds to 36 valence electrons per unit cell and shows a significantly high DOS value. This is indicative of unfavorable electronic structure at the given electron count [40]. However, there is a local minimum at ca. 0.5 eV, and a deep pseudogap at ca. 1 eV above the Fermi level, which correspond to ca. 38 e^-/cell and ca. 40 e^-/cell, respectively. Our refined formulas give ca. 38.6 e^-/cell for $Eu_2Li_{1.36}In_{0.64}Ge_3$, ca. 37.8 e^-/cell for $Eu_2Li_{1.11}Mg_{0.89}Ge_3$, and ca. 38.2 e^-/cell for $Sr_2Li_{1.45}In_{0.55}Ge_3$, respectively. These numbers, together with our unsuccessful attempts to synthesize pure ternary $A_2Li_2Ge_3$ phases (see Experimental), suggest that the "2-2-3" structure does require at least 38 valence electrons per unit cell to attain energetic stability. Coincidentally, the deep pseudogap corresponding to 40 e^- indicates an optimum number of valence electrons, achieved in the archetype $Ce_2Li_2Ge_3$ [35]. Indeed, we have recently synthesized several other isostructural compounds using trivalent lanthanide cations, and the results of these investigations will be discussed in a forthcoming article.

Lastly, a quick recap on Ge–Ge and Li–Ge bonding with regard to the computed COHP curves (Fig. 5, middle and right). Two Ge1–Ge1 COHP curves in the middle of the figure (Ge2 is isolated) display antibonding characters at the Fermi level. Beyond 1 eV, the antibonding character of both Ge1–Ge1 interactions increase significantly. Notice that these calculations underscore a subtle but important difference between the *cis*- and *trans*-interactions, namely, that the *trans*-bonds are a bit shorter (Table 4). This can be understood by recognizing that the *trans*- is slightly less populated than the *cis*-conformation, corresponding to a decrease of its antibonding character (causing the shortening of this bond). Ge1–Li COHP curves display antibonding character at the Fermi level. However, the antibonding character is compensated by the strong bonding character of the Ge2–Li interactions, which remain bonding character up to ca. 1 eV above the Fermi level, and then become nearly nonbonding (longer bond) or even slightly antibonding (shorter bond) above this point.

4. Conclusions

We have successfully synthesized and characterized several $A\mathrm{Li}_{1-x}\mathrm{In}_x\mathrm{Ge}_2$ (A=Sr, Ba, Eu) and $A_2(\mathrm{Li}_{1-x}\mathrm{In}_x)_2\mathrm{Ge}_3$ / $A_2(\mathrm{Li}_{1-x}\mathrm{Mg}_x)_2\mathrm{Ge}_3$ phases (A=Sr, Eu). Both structures contain 1-dimensional $^1_\infty[\mathrm{Ge}_2]$ chains with basic repeating units of $(ct)_n$. Li atoms take a "zwitter" role by participating in covalent interactions with the germanium chains, as well as acting as cations, which transfer their valence electrons to the anionic frameworks. In most compounds, appreciable mixing of Li with either an In or an Mg occurs, modifying the total valence electron count to nearly optimal values. Theoretical investigations revealed that this addition of electrons makes the crystal structures energetically more favorable.

Acknowledgments

Svilen Bobev acknowledges financial support from the National Science Foundation through a Grant DMR-0743916 (CAREER) and from the University of Delaware Research Foundation (UDRF).

Appendix A. Supplementary material

Supplementary data associated with this article (additional crystallographic information, DOS and COHP plots for LT-LaGe) can be found in the online version at doi:10.1016/j.jssc.2010.09.041.

References

[1] T.-S. You, P.H. Tobash, S. Bobev, Inorg. Chem. 49 (2010) 1773.
[2] T.-S. You, S. Bobev, J. Solid State Chem. 183 (2010) 1258.
[3] Q.-X. Xie, R. Nesper, 9thEuropean Conference on Solid State Chemistry, P016, Stuttgart, Germany, 2003.
[4] [a] Q.-X. Xie, R. Nesper, Z. Kristallogr. - New Cryst. Struct 219 (2004) 79; [b] Q.-X. Xie, R. Nesper, Z. Anorg. Allg. Chem. 632 (2006) 1743.
[5] [a] O.K. Andersen, Phys. Rev. B 12 (1975) 3060; [b] O.K. Andersen, O. Jepsen, Phys. Rev. Lett. 53 (1984) 2571; [c] O.K. Andersen, Phys. Rev. B 34 (1986) 2439.
[6] J.T. Vaughey, G.J. Miller, S. Gravelle, E.A. Leon-Escamilla, J.D. Corbett, J. Solid State Chem. 133 (1997) 501.
[7] V.V. Pavlyuk, V.K. Bel'skii, O.I. Bodak, V.K. Percharskii, Dopov. Akad. Nauk B 10 (1987) 45.
[8] J.-G. Mao, Z.-H. Xu, A.M. Guloy, Inorg. Chem. 40 (2001) 4472.
[9] W. Müller, H. Schäfer, A. Weiss, Z. Naturforsch., B 26 (1971)) 534.
[10] Bruker, in: SMART, Bruker AXS Inc., Madison, Wisconsin, USA, 2002.
[11] Bruker, in: SAINT, Bruker AXS Inc., Madison, Wisconsin, USA, 2002.
[12] G.M. Sheldrick, in: SHELXTL, University of Göttingen, Germany, 2001.
[13] G.M. Sheldrick, in: SADABS, University of Göttingen, Germany, 2003.
[14] The very low In content in $\mathrm{BaLi}_{0.99(1)}\mathrm{In}_{0.01}\mathrm{Ge}_2$ cannot be verified independently, however there is a circumstantial evidence that supports such refined formula—DiSalvo group reported stoichiometric BaLiGe_2 [15], the unit cell volume of which is 403.4(1) Å^3 vs. 407.8(4) Å^3 in our case.
[15] D.G. Park, Y. Dong, F.J. DiSalvo, J. Alloys Compd. 470 (2009)) 90.
[16] L.M. Gelato, E. Parthe, J. Appl. Crystallogr. 20 (1987)) 139.
[17] O. Jepsen, A. Burkhardt, O.K. Andersen, in: The TB-LMTO-ASA Program, version 4.7, Max-Planck-Institut für Festkorperforschung, Stuttgart, Germany, 1999.
[18] O.K. Andersen, O. Jepsen, D. Glötzel, in: F. Bassani, F. Fumi, M. Tosi (Eds.), Highlights of Condensed Matter Theory, Lam- brecht, W. R. L., NewYork, North-Holland, 1985.
[19] O. Jepsen, O.K. Anderson, Z. Phys. B 97 (1995) 35.
[20] O.K. Anderson, O. Jepsen, Phys. Rev. Lett. 53 (1984) 2571.
[21] R. Dronskowski, P. Blöchl, J. Phys. Chem. 97 (1993) 8617.
[22] P.E. Blöchl, O. Jepsen, O.K. Anderson, Phys. Rev. B 49 (1994) 16223.
[23] S. Wengert, R. Nesper, Inorg. Chem. 39 (2000) 2861.
[24] P. Villars, L.D. Calvert (Eds.), Pearson's Handbook of Crystallographic Data for Intermetallic Compounds, second ed., American Society for Metals, Materials Park, OH, USA, 1991 and the desktop edition 1997.
[25] B. Chabot, H.F. Braun, K. Yvon, E. Parthe, Acta Crystallogr. B 37 (1981) 668.
[26] H.-J. Mattausch, A. Simon, Z. Naturforsch., B 59 (2004) 519.
[27] E.I. Gladyshevskii, N.S. Uhryu, Dopov. Akad. Nauk 10 (1965) 1326.
[28] F. Merlo, M.L. Fornasini, J. Less-Commom Met. 13 (1967) 603.
[29] L. Pauling, in: The Nature of the Chemical Bond, Cornell University Press, Ithaca, NY, 1960.
[30] S. Bobev, E.D. Bauer, J.D. Thompson, J.L. Sarrao, G.J. Miller, B. Eck, R. Dronskowski, J. Solid State Chem. 177 (2004) 3545.
[31] P.H. Tobash, S. Bobev, J. Solid State Chem. 180 (2007) 1575.
[32] P.H. Tobash, D. Lins, S. Bobev, N. Hur, J.D. Thompson, J.L Sarrao, Inorg. Chem. 45 (2006) 7286.
[33] R.S. Grev, Adv. Organomet. Chem 33 (1991) 125.
[34] B. Pampuch, W. Saak, M. Weidenbruch, J. Organomet. Chem. 693 (2008) 3540.
[35] V.V. Pavlyuk, V.K. Pecharskii, O.I. Bodak, V.A. Bruskov, Sov. Phys. Crystallogr. 33 (1988) 24.
[36] Q.-X. Xie, R. Nesper, Z. Kristallogr. - New Cryst. Struct 219 (2004) 83.
[37] Q.-X. Xie, R. Nesper, Z. Kristallogr. - New Cryst. Struct 218 (2003) 289.
[38] [a] H. Schäfer, Annu. Rev. Mater. Sci. 5 (1985) 1; [b] R. Nesper, Prog. Solid State Chem. 20 (1990) 1; [c] S.M. Kauzlarich (Ed.), Chemistry, Structure and Bonding in Zintl Phases and Ions, VCH, New York, 1996 and the references therein.
[39] For $A\mathrm{Li}_{1-x}\mathrm{In}_x\mathrm{Ge}_2$, obviously, there will be some additional electron density in the conjugated chain (due to the small Li–In admixture), and the formal charge for Ge in those cases will be increased to ca. q=1.55–/1.6–.
[40] G.J. Miller, C.-S. Lee, W. Choe, in: G. Meyer (Ed.), Highlights in Inorganic Chemistry, Wiley-VCH, Heidelberg, 2002, p. 21.